

## Research Article

# Synthesis of Flower-Like $\text{Cu}_2\text{ZnSnS}_4$ Nanoflakes via a Microwave-Assisted Solvothermal Route

Fei Long,<sup>1,2</sup> Shuyi Mo,<sup>1</sup> Yan Zeng,<sup>1</sup> Shangsenshi Chi,<sup>1</sup> and Zhengguang Zou<sup>1,2</sup>

<sup>1</sup> School of Materials Science and Engineering, Guilin University of Technology, Guilin 541004, China

<sup>2</sup> Key Laboratory of Nonferrous Materials and New Processing Technology of Ministry of Education, Guilin University of Technology, Guilin 541004, China

Correspondence should be addressed to Fei Long; [long.drf@gmail.com](mailto:long.drf@gmail.com)

Received 27 January 2014; Revised 6 April 2014; Accepted 8 April 2014; Published 24 April 2014

Academic Editor: Tian-Yi Ma

Copyright © 2014 Fei Long et al. This is an open access article distributed under the Creative Commons Attribution License, which permits unrestricted use, distribution, and reproduction in any medium, provided the original work is properly cited.

Flower-like  $\text{Cu}_2\text{ZnSnS}_4$  (CZTS) nanoflakes were synthesized by a facile and fast one-pot solution reaction using copper(II) acetate monohydrate, zinc acetate dihydrate, tin(IV) chloride pentahydrate, and thiourea as starting materials. The as-synthesized samples were characterized by X-ray diffraction (XRD), Raman scattering analysis, field emission scanning electron microscopy (FESEM) equipped with an energy dispersion X-ray spectrometer (EDS), transmission electron microscopy (TEM), and UV-Vis absorption spectra. The XRD patterns shown that the as-synthesized particles were kesterite CZTS and Raman scattering analysis and EDS confirmed that kesterite CZTS was the only phase of product. The results of FESEM and TEM show that the as-synthesized particles were flower-like morphology with the average size of  $1\sim 2\ \mu\text{m}$  which are composed of 50 nm thick nanoflakes. UV-Vis absorption spectrum revealed CZTS nanoflakes with a direct band gap of 1.52 eV.

## 1. Introduction

$\text{I}_2\text{-II-IV-VI}_4$  quaternary compounds, such as  $\text{Cu}_2\text{ZnSnS}_4$  (CZTS) and  $\text{Cu}_2\text{ZnSnSe}_4$  (CZTSe) based solar cells, exhibit optical and electronic properties comparable to  $\text{Cu}(\text{In, Ga})(\text{S, Se})_2$  (CIGS) and CdTe materials while consisting entirely of nontoxic constituents and avoid the scarcity issues associated with indium, gallium, cadmium, and tellurium. CZTS has a direct band gap of 1.4~1.5 eV and large absorption coefficient in the order of  $10^4\ \text{cm}^{-1}$  [1–3]. Previous reports show that many methods have been utilized for fabricating CZTS thin films, included sputtering [4], electrodeposition [5], coevaporation [6], and coating [7, 8]. The photoelectric conversion efficiency of CZTS-based thin film solar cells has been improved from 0.66% in 1997 [9] to 12.6% in 2013 [10]. Because the narrow thermodynamic window demonstrates that chemical-potential control was important for the growth of high-quality crystals CZTS [11], methods including coevaporation and sputter which obtained high efficiency in CIGS solar cells were not achieved good performance in CZTS thin film solar cells. However, the wet chemical processes based on printing technology have achieved the record

efficiency of CZTS solar cell [10]. Therefore, synthesis of CZTS nanoparticles by hot injection [12], solvothermal [13], hydrothermal [14], and other wet chemical [15] has attracted more attention, and the as-synthesized nanostructures including plate-like [12], sphere-like [13], and spindle-like [16] have been also researched. Although various methods have been utilized to prepare CZTS particles, searching for a simple and rapid synthetic route was still worthy of further exploration. Herein, we report a microwave-assisted solvothermal method to prepare homogeneous and dispersible CZTS flower-like particles from the direct reaction between metal salts and thiourea in ethylene glycol.

## 2. Experimental

*Preparation of the CZTS Particles.* Typically,  $\text{Cu}(\text{CH}_3\text{COO})_2\cdot\text{H}_2\text{O}$  (0.050 M),  $\text{Zn}(\text{CH}_3\text{COO})_2\cdot 2\text{H}_2\text{O}$  (0.025 M),  $\text{SnCl}_4\cdot 5\text{H}_2\text{O}$  (0.025 M), and  $\text{NH}_2\text{CSNH}_2$  (0.200 M) were added in sequence to 30 mL of ethylene glycol at room temperature under magnetic stirring until the chemistries were completely dissolved. Then the mixture was loaded into a Teflon autoclave of 90 mL capacity and putted

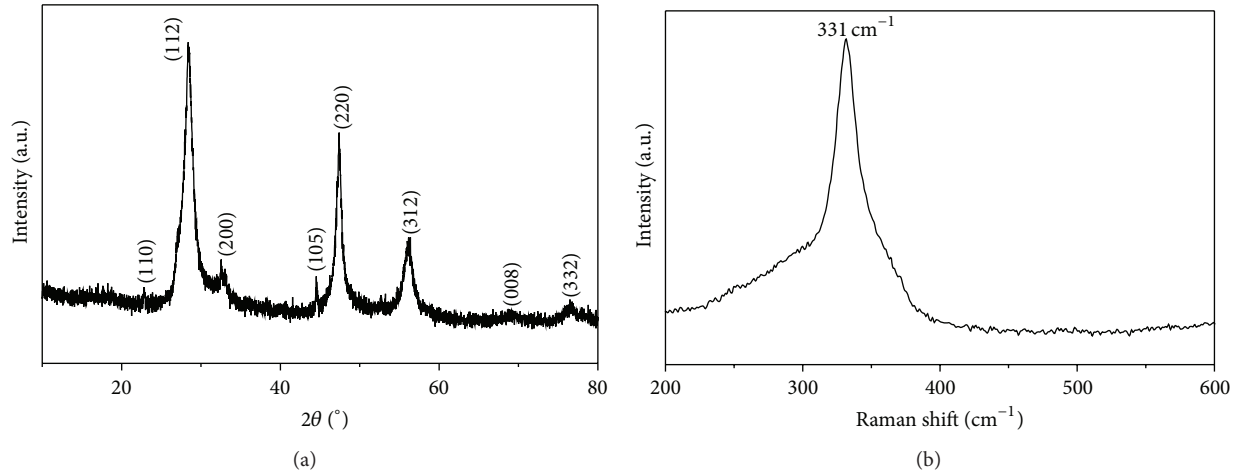


FIGURE 1: (a) XRD pattern of CZTS particles; (b) Raman scattering spectra of CZTS particles; the excitation laser wavelength is 532 nm.

into a microwave oven (2450 MHz, maximum power of 1200 W) heat to 230°C in 10 min and maintained for 1.5 h. The precipitates were centrifuged, washed by deionized water and ethanol for several times to remove by-products, followed by drying in a vacuum chamber at 80°C for 6 h.

**Characterization of the CZTS Particles.** The XRD patterns of as-synthesized particles were obtained on Panalytical X'Pert Pro with Cu K $\alpha$  radiation ( $\lambda = 1.5406 \text{ \AA}$ ) at 35 kV in a scanning range of 10°~80°. Raman spectra were recorded by using Thermo DXR Raman spectrometer at the room temperature, and the 532 nm line of an Ar<sup>+</sup> laser was used as the excitation source. FESEM images were observed by a Hitachi S-4800 field emission scanning electron microscope equipped with an energy dispersion X-ray spectrometer (EDS) and TEM images were recorded on JEOL JSF-2100 at 200 KV. Optical measurements were carried out with Shimadzu UV3600 UV-Vis spectroscopy.

### 3. Results and Discussion

The XRD pattern (Figure 1(a)) of the as-synthesized CZTS particles exhibits that the major XRD diffraction peaks appeared at  $2\theta = 28.44, 47.44$  and  $56.20$  can be attributed to (112), (220), and (312) planes of the CZTS crystals (JCPDS card number 26-0575), respectively. However, the peaks of CZTS XRD patterns were similar to the ZnS (JCPDS card number 65-1691) and Cu<sub>2</sub>SnS<sub>3</sub> (JCPDS card number 27-0198), making it difficult to distinguish between them. So, Raman spectra have been carried out to confirm the products (Figure 1(b)), it exhibits a single intense peak at  $331 \text{ cm}^{-1}$ , which was consistency with previous study [17], and most importantly there was no peak at  $275 \text{ cm}^{-1}$ ,  $352 \text{ cm}^{-1}$ ,  $267 \text{ cm}^{-1}$ ,  $303 \text{ cm}^{-1}$ , and  $365 \text{ cm}^{-1}$  suggest that the products absence of cubic ZnS and Cu<sub>2</sub>SnS<sub>3</sub> [18].

The images of FESEM (Figures 2(a) and 2(b)) indicate that the as-synthesized CZTS particles were monodisperse superstructures with a uniform 3-dimensional flower-like

morphology with the average size of  $1\sim 2 \mu\text{m}$ . Furthermore, these superstructures were built from intersectional nanoflakes with thickness about 50 nm (Figure 2(c)). The average composition of the products was Cu:Zn:Sn:S = 2:0.97:1.02:3.73 base on the result of EDS (Figure 2(d)), the slightly Sn rich and Zn poor composition deviated from stoichiometric may be due to different reactivity of starting materials.

The images of TEM, selected area electron diffraction (SAED), and high resolution transmission electron microscopy (HRTEM) of as-synthesized CZTS particles were shown in Figure 3. The average size of CZTS particles corresponds well with the FESEM images (Figure 2), and the flower-like particles were built from cross-nanoflakes (Figure 3(a)). SAED image reveals the polycrystalline nature of CZTS nanoflakes which was indicated by the presence of diffraction spots of (112), (220), and (312) planes. The HRTEM image of one nanoflake shows the interplanar spacing of  $1.9 \text{ \AA}$  corresponding to the (220) planes.

The UV-Vis absorption spectrum of CZTS particles was shown in Figure 4. We determined the absorbance onset by plotting  $(Ah\nu)^2$  versus  $h\nu$  ( $A$ : absorbance,  $h$ : Planck's constant, and  $\nu$ : frequency). From the long wavelength extrapolation of the band edge, the band gap was determined to be 1.52 eV which was in good agreement with the corresponding bulk materials [1]. This observation also eliminates existence of secondary phase of ZnS and Cu<sub>2</sub>SnS<sub>3</sub>. The good absorption in the visible light region may find its potential application in thin films solar cells.

### 4. Conclusions

Single phase kesterite CZTS has been prepared at 230°C for only 1.5 h via a microwave-assisted solvothermal without any surfactant; the CZTS particles with flower structure built from intersectional nanoflakes have been obtained, Cu:Zn:Sn:S = 2:0.97:1.02:3.73. Its founded microwave has strongly activated the process of solvothermal synthesis which significantly speeds up the reaction compared with

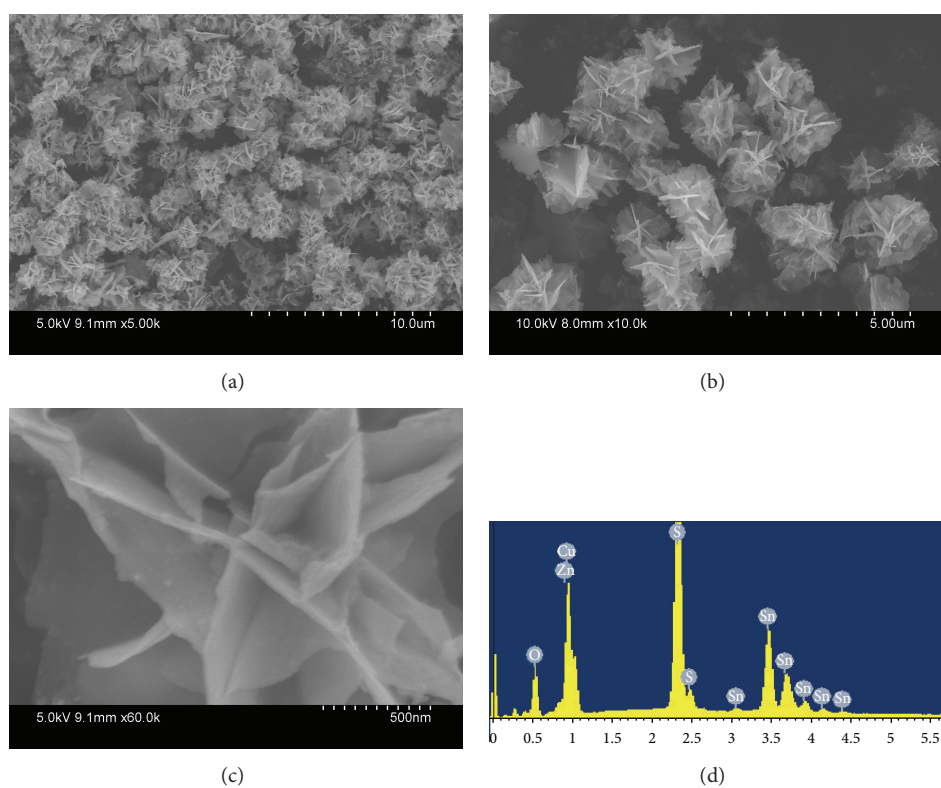


FIGURE 2: (a)–(c) FESEM images of CZTS particles; (d) EDS of CZTS particles.

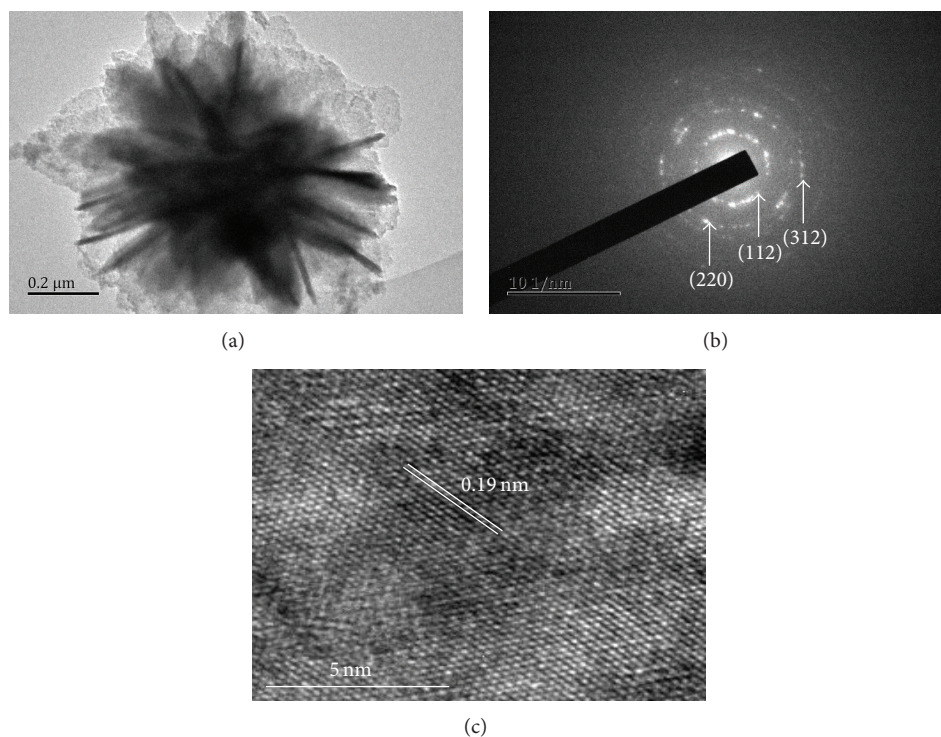


FIGURE 3: (a) TEM images of CZTS particles dispersed in ethanol; (b) SAED pattern; (c) HRTEM image.

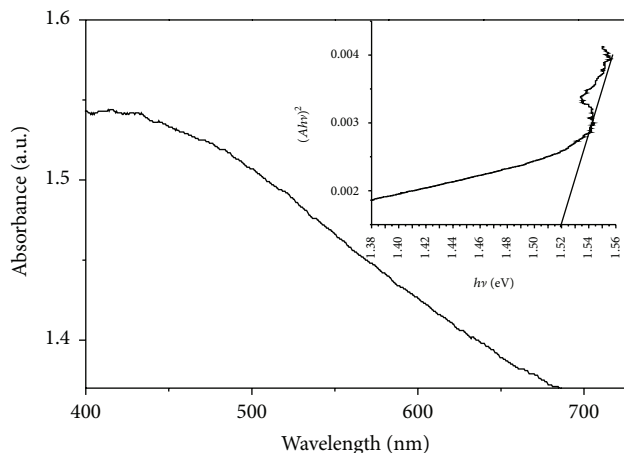


FIGURE 4: UV-Vis absorption spectrum of CZTS particles. The inset image shows a band gap of 1.52 eV.

traditional solvothermal synthetic methods. The UV-Vis absorption spectra of the products revealed that the band gap was 1.52 eV, which is optimal for photovoltaic applications.

## Conflict of Interests

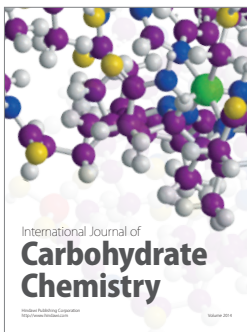
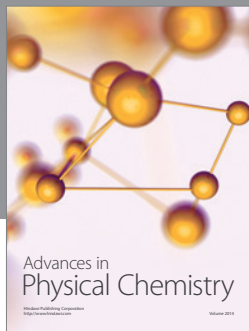
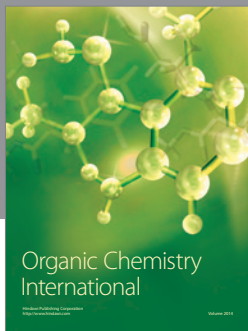
The authors declared that they do not have a direct financial relation with the commercial identities mentioned in this paper that might lead to any conflict of interest for any of the authors.

## Acknowledgments

This work was financially supported by the National Natural Science Foundation of China (no. 51162005), National High-Tech Research and Development Program of China (863 Program, no. 2012AA050704), and Guangxi Natural Science Foundation (2011GXNSFD018007).

## References

- [1] K. Ito and T. Nakazawa, "Electrical and optical properties of stannite-type quaternary semiconductor thin films," *Japanese Journal of Applied Physics*, vol. 27, no. 11, pp. 2094–2097, 1988.
- [2] H. Katagiri, K. Saitoh, T. Washio, H. Shinohara, T. Kurumadani, and S. Miyajima, "Development of thin film solar cell based on  $\text{Cu}_2\text{ZnSnS}_4$  thin films," *Solar Energy Materials and Solar Cells*, vol. 65, no. 1–4, pp. 141–148, 2001.
- [3] H. Matsushita, T. Maeda, A. Katsui, and T. Takizawa, "Thermal analysis and synthesis from the melts of Cu-based quaternary compounds  $\text{Cu-III-IV-VI}_4$  and  $\text{Cu}_2\text{-II-IV-VI}_4$  (II = Zn, Cd; III = Ga, In; IV = Ge, Sn; VI = Se)," *Journal of Crystal Growth*, vol. 208, no. 1–4, pp. 416–422, 2000.
- [4] H. Katagiri, K. Jimbo, S. Yamada et al., "Enhanced conversion efficiencies of  $\text{Cu}_2\text{ZnSnS}_4$ -based thin film solar cells by using preferential etching technique," *Applied Physics Express*, vol. 1, no. 4, Article ID 041201, 2008.
- [5] A. Shafaat, K. B. Reuter, O. Gunawan, L. Guo, L. T. Romankiw, and H. Deligianni, "A high efficiency electrodeposited  $\text{Cu}_2\text{ZnSnS}_4$  solar cell," *Advanced Energy Materials*, vol. 2, no. 2, pp. 253–259, 2012.
- [6] B. Shin, O. Gunawan, Y. Zhu, N. A. Bojarczuk, S. J. Chey, and S. Guha, "Thin film solar cell with 8.4% power conversion efficiency using an earth-abundant  $\text{Cu}_2\text{ZnSnS}_4$  absorber," *Progress in Photovoltaics: Research and Applications*, vol. 21, no. 1, pp. 72–76, 2013.
- [7] D. A. R. Barkhouse, O. Gunawan, T. Gokmen, T. K. Todorov, and D. B. Mitzi, "Device characteristics of a 10.1% hydrazine-processed  $\text{Cu}_2\text{ZnSn}(\text{Se},\text{S})_4$  solar cell," *Progress in Photovoltaics: Research and Applications*, vol. 20, no. 1, pp. 6–11, 2012.
- [8] Q. Guo, G. M. Ford, W.-C. Yang et al., "Fabrication of 7.2% efficient CZTS solar cells using CZTS nanocrystals," *Journal of the American Chemical Society*, vol. 132, no. 49, pp. 17384–17386, 2010.
- [9] H. Katagiri, N. Sasaguchi, S. Hando, S. Hoshino, J. Ohashi, and T. Yokota, "Preparation and evaluation of  $\text{Cu}_2\text{ZnSnS}_4$  thin films by sulfurization of E-B evaporated precursors," *Solar Energy Materials and Solar Cells*, vol. 49, no. 1–4, pp. 407–414, 1997.
- [10] W. Wang, M. T. Winkler, O. Gunaman et al., "Device characteristics of CZTS thin-film solar cells with 12.6% efficiency," *Advanced Energy Materials*, 2013.
- [11] A. Walsh, S. Chen, S. H. Wei, and X. G. Gong, "Kesterite thin-film solar cells: advances in materials modelling of  $\text{Cu}_2\text{ZnSnS}_4$ ," *Advanced Energy Materials*, vol. 2, no. 4, pp. 400–409, 2012.
- [12] H. Wei, W. Guo, Y. Sun, Z. Yang, and Y. Zhang, "Hot-injection synthesis and characterization of quaternary  $\text{Cu}_2\text{ZnSnSe}_4$  nanocrystals," *Materials Letters*, vol. 64, no. 13, pp. 1424–1426, 2010.
- [13] Y.-L. Zhou, W.-H. Zhou, Y.-F. Du, M. Li, and S.-X. Wu, "Sphere-like kesterite  $\text{Cu}_2\text{ZnSnS}_4$  nanoparticles synthesized by a facile solvothermal method," *Materials Letters*, vol. 65, no. 11, pp. 1535–1537, 2011.
- [14] C. C. Kang, H. F. Chen, T. C. Yu, and T. C. Lin, "Aqueous synthesis of wurtzite  $\text{Cu}_2\text{ZnSnS}_4$  nanocrystals," *Materials Letters*, vol. 96, pp. 24–26, 2013.
- [15] J. J. Li, J. Shen, Z. Q. Li et al., "Wet chemical route to the synthesis of kesterite  $\text{Cu}_2\text{ZnSnS}_4$  nanocrystals and their applications in lithium ion batteries," *Materials Letters*, vol. 92, pp. 330–333, 2013.
- [16] W. Ming, Q. Y. Du, D. C. Wang, W. F. Liu, G. S. Jiang, and C. F. Zhu, "Synthesis of spindle-like kesterite  $\text{Cu}_2\text{ZnSnS}_4$  nanoparticles using thiorea as sulfur source," *Materials Letters*, vol. 79, pp. 177–179, 2012.
- [17] S. R. Kumar, B. D. Ryu, S. Chandramohan, J. K. Seol, S. K. Lee, and C. H. Hong, "Rapid synthesis of sphere-like  $\text{Cu}_2\text{ZnSnS}_4$  microparticles by microwave irradiation," *Materials Letters*, vol. 86, pp. 174–177, 2012.
- [18] P. A. Fernandes, P. M. P. Salomé, and A. F. da Cunha, "Study of polycrystalline  $\text{Cu}_2\text{ZnSnS}_4$  films by Raman scattering," *Journal of Alloys and Compounds*, vol. 509, no. 28, pp. 7600–7606, 2011.



**Hindawi**

Submit your manuscripts at  
<http://www.hindawi.com>

